Quaternary Science Reviews 257 (2021) 106864

Contents lists available at ScienceDirect

Quaternary Science Reviews

journal homepage: www.elsevier.com/locate/quascirev

The role of wetland expansion and successional processes in methane emissions from northern wetlands during the Holocene

Claire C. Treat [a, b, d, *], Miriam C. Jones [c], Laura Brosius [a], Guido Grosse [d, e], Katey Walter Anthony [a], Steve Frolking [b]

[a] Water and Environmental Research Center, Institute for Northern Engineering, University of Alaska Fairbanks, Fairbanks, AK, 99775, USA
[b] Institute for the Study of Earth, Oceans & Space, University of New Hampshire, Durham, NH, 03824, USA
[c] U.S. Geological Survey, Reston, VA, 20192, USA
[d] Alfred Wegner Institute Helmholtz Centre for Polar and Marine Research, 14473, Potsdam, Germany
[e] University of Potsdam, Institute of Geosciences, 14476, Potsdam, Germany

ARTICLE INFO

Article history:
Received 22 September 2020
Received in revised form
18 February 2021
Accepted 21 February 2021
Available online xxx

Handling Editor: Yan Zhao

Keywords:
Methane
Wetland
Peatland
Holocene
Bog
Permafrost

ABSTRACT

The contribution from northern high latitude wetlands are a major uncertainty in the atmospheric methane (CH_4) budget throughout the Holocene. We reconstructed CH_4 emissions from northern peatlands from 13,000 BP to present using an empirical model based on observations of peat initiation (>3600 dates), peatland type (>250 peat cores), and observed CH_4 emissions in order to explore the effects of changes in wetland type on CH_4 emissions over the end of the late glacial and the Holocene. Fen area increased steadily before 8000 BP as fens formed in major wetland complexes. After 8000 BP, new fen formation continued but widespread peatland succession (to bogs) and permafrost aggradation occurred. Reconstructed CH_4 emissions from peatlands increased rapidly between 10,600 BP and 6900 BP due to fen formation and expansion. Emissions stabilized after 5000 BP at 42 ± 25 Tg CH_4 y^{-1} as high-emitting fens transitioned to lower-emitting bogs and permafrost peatlands. Widespread permafrost formation in northern peatlands after 1000 BP decreased CH_4 emissions by 20%–34 ± 21 Tg y^{-1} by the present day and suggests peatland CH_4 emissions will increase with permafrost thaw.

1. Introduction

Dynamic changes in atmospheric methane (CH_4) concentrations since the onset of deglaciation are recorded in ice cores, with rapid increases observed in both Greenland and Antarctic ice cores at during the Bølling-Allerød (14.7 ka (ka = 1000 years BP)) and the Younger Dryas-Preboreal transition at 11.6 ka (Blunier et al., 1995; Bock et al., 2017; Brook et al., 2000). The changes in atmospheric CH_4 concentrations predominantly reflect the changes in natural biological sources during this period, including wildfire, northern and tropical wetlands, permafrost thaw, lake formation, and others (Petrenko et al., 2017). Atmospheric scientists have used atmospheric modeling of CH_4 sources and sinks aimed at matching the observed shifts in the interpolar gradient of CH_4 concentrations, as well as in stable and radioactive isotopes of CH_4, in ice cores to partition the magnitude of the various possible CH_4 sources (Beck et al., 2018; Bock et al., 2017; Brook et al., 2000; Petrenko et al., 2009, 2017; Sowers, 2010). However, the magnitudes of individual sources and drivers of change remain uncertain and represent an area of vigorous debate (Bock et al., 2017; Dyonisius et al., 2020; Petrenko et al., 2017).

The expansion of northern high latitude peatlands following ice sheet retreat and the transition to a wetter, warmer climate is thought to have contributed substantially to the increase in atmospheric CH_4 concentrations during the deglacial and Holocene (MacDonald et al., 2006; Jones and Yu, 2010). Today, peatland complexes cover more than 3.1 × 10^6 km^2 in northern high latitudes (Hugelius et al., 2020) and emit an estimated 30 Tg CH_4 yr^{-1} (Frolking et al., 2011), making them an important component of northern wetland emissions. The formation of northern peatlands (Jones and Yu, 2010; MacDonald et al., 2006) and permafrost thaw lakes (Walter et al., 2007) coincides with the rapid increases in atmospheric CH_4 at the end of the Younger Dryas, but others have

* Corresponding author. Permafrost Research Section, Alfred Wegener Institute Helmholtz Centre for Polar and Marine Research, Telegrafenberg A45, 14473, Potsdam, Germany.
E-mail address: Claire.treat@awi.de (C.C. Treat).

https://doi.org/10.1016/j.quascirev.2021.106864

proposed increases in tropical wetland sources as the dominant CH_4 source in the early Holocene (Bock et al., 2017; Singarayer et al., 2011). Nevertheless, understanding how CH_4 emissions from northern peatlands responded to climatic changes in the past provides valuable insight for understanding how emissions of this important greenhouse gas will change with a rapidly warming climate.

Peatlands are wetlands that accumulate organic soils (peat) because vegetation productivity exceeds decomposition, preserving a record of the timing of their development in the basal organic sediments. Using radiocarbon ages of basal peats, spatial and temporal estimates of peat accumulation and peatland expansion have been made across northern high latitudes (Gorham et al., 2007; Korhola et al., 2010; MacDonald et al., 2006; Nichols and Peteet, 2019). Peatlands often initiate as fens, which are defined by their connection to groundwater, but often accumulate peat above the groundwater table with time, resulting in a transition to a precipitation-fed bog. The stratigraphic accumulation of peat provides a time series of peatland development using the composition of plant macrofossils within the peat and comparing the species composition assemblages to present-day vegetation communities which can be used to reconstruct the evolution of wetland types through time (Charman, 2002; Mauquoy et al., 2010). Wetland and peatland types often change over time as a result of ecosystem succession, long-term climate change, and permafrost aggradation and thaw (Treat et al., 2016). Reconstructions of peatland and wetland type have been used both at a site level to examine local responses to climatic drivers (Kuhry et al., 1992), and at larger, regional scales to understand responses to broader climate drivers (Treat and Jones, 2018).

From a greenhouse gas perspective, large-scale changes among wetland types with different hydrologic regimes and productivity levels may have altered the net CH_4 emissions from wetlands during the Holocene (Mathijssen et al., 2016; Yu et al., 2013). One particularly important change is from fens to bogs, which occurs relatively frequently in northern peatlands as peat accumulates above the groundwater level (Treat et al., 2016). This shift generally results in lower CH_4 emissions (Treat et al., 2018) and alters the $\delta^{13}C{-}CH_4$ due to differences in dominant CH_4 production pathways between the two peatland types (Hornibrook, 2009). In the global CH_4 budget during the Holocene, decreases in northern hemisphere CH_4 sources and shifts in $\delta^{13}C{-}CH_4$ between 11 ka to 8 ka have been attributed to the transition from fens to bogs in northern peatlands (Beck et al., 2018). However, this assumption of fen-bog transitions during this period has yet to be tested using observations of peatland types from paleoecological records across broad spatial scales.

In addition to differences in the stable isotopes of CH_4, flux rates also differ among peatland types. Methane flux rates are the net of two different processes: CH_4 production from the anaerobic decomposition of organic matter in saturated soils, and CH_4 oxidation in overlying unsaturated soils. Wetland type can be a good predictor of net CH_4 flux rates because of the correlation with plant community composition, which can represent underlying differences in productivity, carbon availability, redox status, and water table position (Blodau, 2002; Bubier, 1995; Treat et al., 2018). Because of these differences, CH_4 flux rates from early successional stage peatlands, such as marshes and fens, can be 50%–700% greater than from later stage bogs (Treat et al., 2018). Soil temperature is also an important control on CH_4 emissions through controlling rates of microbial processes and is particularly important for predicting intra-annual flux dynamics (Chadburn et al., 2020). Permafrost presence or absence is an important predictor of annual CH_4 emissions, with 200%–1500% larger emissions from permafrost-free peatlands than from permafrost peatlands (Treat et al., 2018). Therefore, capturing these key differences in CH_4 flux among different wetland types and permafrost presence/absence is key to understanding CH_4 emissions over time.

In this study, we used several different data-based syntheses to reconstruct northern peatland types, areas, and CH_4 emissions continuously from the Younger Dryas through the Holocene. We reconstructed total northern peatland areas using a synthesis of extant (found in present-day) peatland basal ages and partitioned the areas into nine wetland types including peatlands and other wetlands that later formed peats using a classification from a synthesis of paleoecological reconstructions based on plant macrofossil analysis. We then matched the reconstructed area of each wetland type with their corresponding present-day CH_4 flux rates using an extensive synthesis of wetland CH_4 flux rates in order to reconstruct CH_4 emissions from northern wetlands over time. The goal of this study was to make a first-order estimate of CH_4 emissions throughout the Holocene associated with northern peatland formation, expansion, succession, and permafrost dynamics from existing northern peatland areas using the best information available.

2. Methods

We reconstructed CH_4 emissions from extant (found in present-day) northern peatlands from 13 ka through the Holocene using several observationally-derived datasets: peatland areas based on ^{14}C dated records of peatland initiation (>3600 basal ages), peatland type based on paleoecological analysis of 262 chronologically-constrained peat cores from across northern high latitudes, and CH_4 fluxes based on an extensive synthesis of contemporary annual emissions from 256 site-years across 101 sites (Fig. 1). This approach captures many wetlands areas over time when they eventually form peat, but using peatlands as a proxy for all wetland areas excludes some wetlands such as seasonally-inundated wetlands and some open-water wetland, marshes, and swamps that do not form peat. To clarify that we are limiting this study to present-day peatland areas, rather than non-peat-forming (mineral soil) wetlands or peatlands no longer on the landscape today, we use "peatland area" and "peatland CH_4 emissions" throughout this study, even if referring to wetland types that were not technically peatlands, such as shallow water wetlands and some marshes that later developed into and are now peatlands. The northern peatland study region that we used was the LGM permafrost region (Lindgren et al., 2015; Vandenberghe et al., 2014), an area that would likely have strong peatland formation in deglacial and thermokarst landscapes.

2.1. Peatland expansion and succession

To reduce sampling bias from proximity to peatland researchers (e.g. Fig. 1), we determined permafrost and permafrost-free peatland areas separately for each region shown in Fig. 1 using the basal ages from each region. Present day peatland areas (A) were determined from soil maps using the total areas classified as "histosol" (peatlands) and "histel" (permafrost peatlands) within each region (Table 1; Hugelius et al., 2020). Peatland basal ages (B) were from Treat et al. (2019) (Fig. 1) and are available on Pangaea (https://doi.org/10.1594/PANGAEA.873065, Table S2). Basal ages were divided into 100-year age bins based on the median calibrated radiocarbon age using IntCal13 (Reimer et al., 2013).

The reconstruction of past peatland extent (area) was based on cumulative density functions of the fraction of total peat basal dates and present-day peatland extent. Peatland areas (A) were calculated for time (t) by summing over 100-year age bins as:

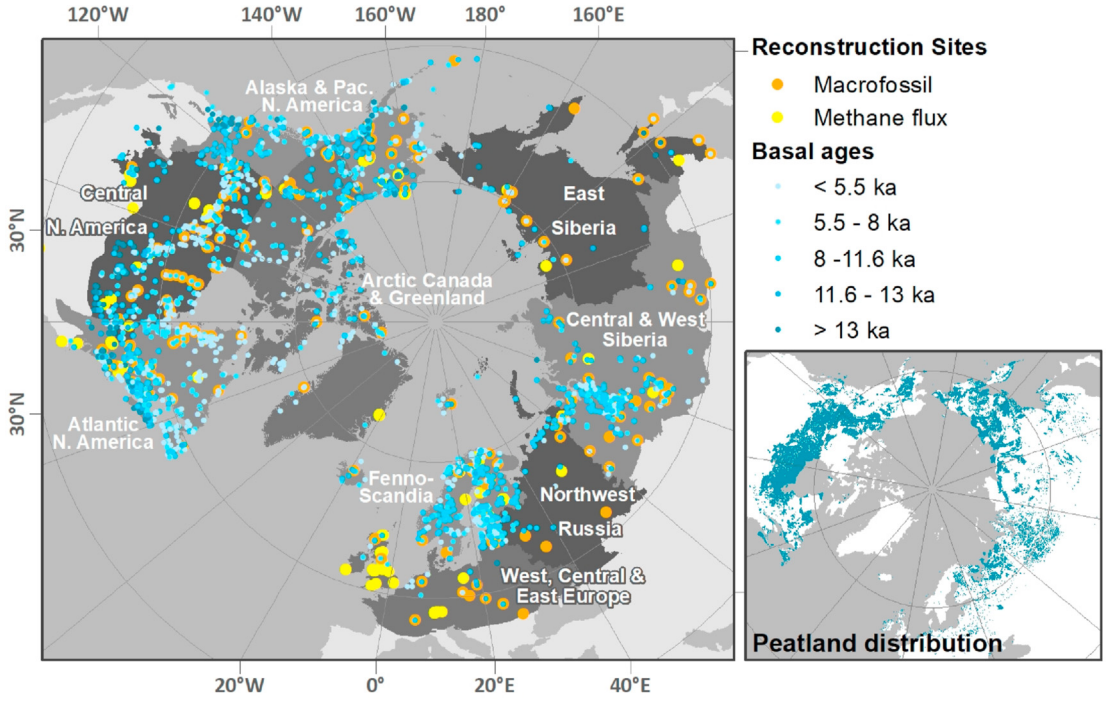

Fig. 1. Map of the datasets and regions used in this study. Locations of peatland initiation dates (blue circles), peat macrofossil cores used in the reconstruction of peatland classifications (orange circles), and CH_4 flux measurements (yellow circles). The dark gray colors represent the regions used within the reconstruction and the study domain extent, with the southern limit defined as the LGM permafrost region (Lindgren et al., 2015; Vandenberghe et al., 2014). Latitude grid represents 30 °N, 50 °N, and 70 °N. Inset: current peatland areas (blue) from (Xu et al., 2018). (For interpretation of the references to color in this figure legend, the reader is referred to the Web version of this article.)

Table 1
Present-day peatland areas, permafrost peatland areas, and number of samples from each peatland region (Fig. 1). Regions are shown in Fig. 1. Regional areas and percentage of permafrost area are adapted from Hugelius et al. (2020). Basal ages from Treat et al. (2019); macrofossil data is also described in Treat and Jones (2018). Abbreviations: N: number of samples; PF: permafrost found in core in present-day; macro cores: peat cores with ^{14}C-dated macrofossil analysis.

Region name	Total Peatland Area (10^3 km^2)	Permafrost Area (%)	N basal ages	N macro cores (no PF)[a]	N macro cores (with PF)
Alaska & Pacific North America	199	53	520	21	5
Arctic Canada & Greenland	260	89	346	2	29
Atlantic North America	204	4	791	25	22
Central North America	874	26	689	31	25
East Siberia	326	85	66	8	16
Fenno-Scandia	245	14	724	11	3
Northwest (European) Russia	274	65	55	5	11
West & Central Siberia	870	49	283	18	6
West, Central, and East Europe	151	1	104	16	0
Total	**3403**	**44**	**3612**	**137**	**117**

[a] Includes 4 cores in Central North America and 2 cores in West Siberia with unknown permafrost status.

$$A_t = \frac{\sum_{t_{init}}^{t} B_t}{B} \times A_{t_0}. \quad (1)$$

where the first term represents the cumulative density function. Here, B_t is the number of peatlands that have formed at time t as indicated by their basal age being that age or older, B is the sum of B_t from t_{init} to t_0, t_{init} represents the oldest basal age in the database (t_{init} = 21 ka), and t_0 is present-day. This approach assumes that maximum peatland extent is reached during the present day and excludes now-buried peatlands (Treat et al., 2019).

To determine the areas of each peatland type, we identified wetland types from peat cores by using plant macrofossils and other physical indicators. We selected cores from a large synthesis macrofossil dataset (Treat and Jones, 2018; Treat et al., 2016) that met all of the following criteria: 1) they contained the entire peat profile from the surface to underlying mineral soils and a minimum of 20 cm of peat; 2) they had relatively high dating resolution of more than one date per 2000 years; 3) they had detailed macrofossil analysis that could be used to classify the peat type over time; 4) they fell within the LGM permafrost region (Lindgren et al., 2015; Vandenberghe et al., 2014), an area that would likely have strong peatland formation in deglacial and thermokarst landscapes (Treat et al., 2019; Walter Anthony et al., 2014). These selection criteria resulted in 10,630 records of plant macrofossils and chronologies from 262 peatland cores (Fig. 1). In the present day, 44 cores were from permafrost-free fens, 82 cores were from permafrost-free bogs, 3 were from permafrost-free marshes and swamps, and 117 were from permafrost peatlands.

We categorized these plant macrofossil records into wetland classes defined by the Canadian Wetland Classification system (National Wetlands Working Group, 1988) using the methods described in Treat et al. (2016). The categories included both peatlands (swamps, rich fens, fens, poor fens, bogs, permafrost bogs

and peat plateaus, tundra peatlands with permafrost, thawed permafrost peatlands), and non-peat-forming ecosystems that later formed peat (shallow water wetlands, marshes, as well as lakes and rivers, lagoons, permafrost thaw ponds, and uplands). Because these wetland sites eventually formed peatlands, we refer to all stages as "peatland" here to distinguish these wetlands from non-peat forming wetlands found in the present day. For each core, the classification of peatland type was converted from a depth scale to an age scale using core-specific age-depth models developed from core chronologies using BACON (Blaauw and Christen, 2011; Treat and Jones, 2018) on calibrated radiocarbon ages (Reimer et al., 2013). The site locations and references are included in Table S1. Other information in the macrofossil dataset including plant macrofossils, peat properties, and core chronologies is available on PANGAEA (doi: 10.1594/PANGAEA.863697).

We partitioned the peatland areas (Equation (1)) into peatland-class specific areas using the peat categories from the macrofossil cores described above. The macrofossil cores were separated by region and permafrost presence at the site in the present day and were assumed to be representative of wetland development through time within each region. Using the same cores as this study, Treat and Jones (2018) showed that patterns of peatland development were often similar within these same regions and often correlated with external climatic drivers, providing support for this assumption. We calculated the areas of each peatland type through time using:

$$A_{j,t} = A_t \times \frac{P_{j,t}}{P_t} \quad (2)$$

Where P is the number of macrofossil peat cores at time t, and j is the peatland classification derived from the peat core reconstruction. These calculations were done separately for permafrost-free peatland areas and permafrost peatland areas (Table 1) using cores without and with permafrost in the present-day, respectively. In cases where peat basal ages indicated existing peatland area within a region but there were no macrofossil records from which to determine peatland type, we assumed that the oldest available records of the peatland types were representative of peatlands that formed earlier. The development of the small area of permafrost peatlands in West, Central, and Eastern Europe were assumed to follow the developmental history of permafrost cores in Fennoscandia.

2.2. Peatland CH_4 emissions modeling

Northern peatland CH_4 emissions depend on peatland type and area of that peatland type. Methane fluxes were modeled using:

$$F_t = \sum_{j=1}^{j=n} A_{j,t} \times F_{j0}. \quad (3)$$

where F_t is total northern wetland CH_4 emissions at time t, $A_{j,t}$ is the peatland area at time t of peatland type j derived from the peat core reconstruction (Eq. (2)), and F_{j0} is the type-specific annual CH_4 flux in the present day for each wetland and peatland type (Table 2), which were determined from an extensive literature review of annual CH_4 flux measurements that includes non-growing season measurements (Treat et al., 2018). While this approach assumes that past CH_4 fluxes were analogous to today, we discuss below factors that might contribute to non-analogous CH_4 flux and how this would change the total wetland CH_4 flux.

2.3. Uncertainties in peatland areas and CH_4 flux

We quantified uncertainties in the peatland areas associated with basal ages and present-day peatland mapping. To quantify uncertainty associated with basal ages, we used bootstrap resampling to sample from a normal distribution centered on the median calibrated date and constrained by the two-sigma ages on the tails. We aggregated these results across each study region to get the cumulative distribution of basal ages, repeated 500 times, and calculated the mean number of newly formed peatlands and 95% confidence intervals. We repeated the area calculation (Eq. (1)) using the minimum and maximum of the 95% confidence intervals. Uncertainties due to peatland mapping were calculated using the mapping uncertainty of the present-day peatland area (500,000 km^2; Hugelius et al., 2020) and were assumed to be constant over time. We assumed independence of the two sources of uncertainty on the area and summed these error terms to calculate total area uncertainty.

Uncertainties in CH_4 flux were calculated from the independent uncertainties on areal CH_4 flux rates and area (Eq. (2) and (3)). Uncertainties in the median peatland CH_4 flux across all classes and for each class were determined using bootstrap resampling with replacement (R command: sample) with 1000 replicates. We took the mean of the median CH_4 flux across the 1000 replicates and the 95% confidence intervals for each of the peatland classes (Table 2; Equation (3)).

3. Results

3.1. Trends in peatland and wetland composition and extent since 13 ka

Peatland basal ages indicate that peatland initiation occurred across the study region following the beginning of deglaciation. Before 13 ka, the majority of peatland initiation occurred in North America, with only a few dates indicating peatland formation in Eurasia (Fig. 1). Peatland initiation rates decreased between 13 ka and 12 ka, corresponding to cooling during the Younger Dryas (Fig. 2a). Following the end of the Younger Dryas and the beginning of the Holocene, peat basal ages indicate a strong increase in peatland formation in Fennoscandia and West and Central Siberian regions, particularly in the West Siberian Lowlands (Fig. 1), with the most rapid rates of peat initiation occurring across northern high latitudes between 10 ka to 7.5 ka. After 7.5 ka, rates of peatland initiation in Central and Eastern North America increased as peatlands formed in Western Canada, and the Hudson Bay and James Bay Lowlands, while the formation of new peatlands in West and Central Siberia was limited (Fig. 1). Overall rates of peatland initiation have been decreasing over the past 4 ka (Fig. 2a).

The earliest records of peatland type from plant macrofossil records in peat cores show that, prior to 10 ka, most sites were shallow water wetlands, marshes, or swamps (20–45%) and fens (20–50%) (Fig. 2b and c). Fens were common in Alaska during the early part of these records, while shallow water wetlands, marshes, and swamps and other water bodies (pre-peat) were common across the rest of the study domain (Fig. 3). The number and percentage of records indicating fen peatland type increased strongly between 12 ka and 7 ka, when 60–70% of all the peat cores at the time indicated fen-type peatland vegetation assemblages (Fig. 2c). Records of bogs were rare at 10 ka (Figs. 2 and 3), with only a few sites in the showing evidence of these wetland types in Central Europe and North Western Siberia. While shallow water wetlands, marshes, and swamps made up a large percentage of cores prior to

Table 2
Median methane fluxes (g CH_4 m^{-2} y^{-1}) to the atmosphere from northern peatlands, and 95% confidence intervals around the median. Recalculated from Treat et al. (2018). Peatland class represents the categories used in reconstruction (plant macrofossil analysis and CH_4 flux calculations), while the aggregate classes (in parentheses) are shown in figures and include the sum of the individual peatland classes. CI: confidence interval.

Peatland class (Aggregate class)	Median CH_4 flux	(upper − lower 95% CI)	n
Shallow Water (Shallow + Marsh + Swamp)	35.8	(+5.8 − +65.9)	11
Marsh (Shallow + Marsh + Swamp)	46.4	(+25.7 − +67.2)	24
Swamp (Shallow + Marsh + Swamp)	19.9	(+0.0 − +50.9)	13
Fen (Fen)	24.2	(+18.5 − +29.8)	45
Poor Fen (Fen)	27.0	(-3.7 − +57.6)	16
Rich Fen (Fen)	13.0	(+4.6 − +21.7)	16
Bog (Bog)	5.7	(+2.3 − +9.3)	37
Peat plateau & palsa (Permafrost)	2.9	(+0.4 − +5.4)	18
Tundra peat (permafrost) (Permafrost)	4.1	(+2.1 − +6.2)	30
Permafrost thaw (not shown)	23.8	(+11.4 − +36.2)	13

10 ka, these peatland types were only a small fraction (<10%) of the samples during the rest of the Holocene.

After 7.5 ka, the number and fraction of peat cores indicating bog-type peatland vegetation assemblages increased strongly, from ~10 cores to nearly 80 cores by modern times (0 ka), or from about 10% of the cores to 30% of the cores (Figs. 2d and 3). A regional pattern of fen-bog transition appeared by 7.5 ka in Europe and the UK, while only a few isolated sites in North America indicated bog development at 7.5 ka (Fig. 3). Widespread fen-bog transitions appeared in records from the Atlantic Coast of North America, Northwestern Canada, and the Baltic region by 5ka. By 2.5 ka, the transition from fens to bogs on the Atlantic Coast of North America was nearly complete and the fen-bog transition rate had accelerated in Western Canada (Fig. 3). By the present-day, most records from Western Canada had developed either into bogs or permafrost wetlands (Fig. 3).

Permafrost aggradation in peatlands was indicated by plant macrofossils after 9 ka, with steady increases in the number of cores with permafrost occurring between 9 ka and 2.5 ka (Fig. 2e). Regional trends in permafrost aggradation are apparent at 7.5 ka in sites relatively close to the Beaufort Sea in Alaska and coastal-adjacent regions of northern Siberia (Fig. 3). By 2.5 ka, permafrost aggradation in peatlands was common in Northwestern Canada and in Northern Siberia (Fig. 3). The rate of permafrost aggradation in peatlands increased slightly after 2.5 ka, and sharply after 1 ka, with permafrost occurring in ~40% of the peat cores sampled from the permafrost region by modern times. A major driver of this trend was the aggradation of permafrost in cores across Western Canada, Alaska, and Northern Siberia (Fig. 3). While the number of cores indicating fen peatland types was stable between ~6 ka and 1 ka due to new peatland initiation and expansion as fens, the widespread transition from fens to bogs and the sharp increase in aggradation of permafrost (Fig. 3) decreased the relative fraction of fens occurring in the permafrost region since 7 ka to about 25% of the cores sampled today (Fig. 2c).

3.2. Changes in peatland area and composition during the Holocene

Assuming that regional peatland development followed the patterns of peatland initiation from the basal ages (Fig. 2a), we modeled relatively small peatland areas prior to the Early Holocene (Fig. 4a). Before 11 ka, we estimate that peatland area comprised less than 10% of present-day peatland area (<300,000 km^2), as most peatlands had yet to form in the major northern peatland areas including Hudson Bay Lowlands, West Siberian Lowlands, and Fennoscandia (Figs. 1 and 4). A period of major wetland formation and expansion occurred between 10.6 ka and 6.9 ka as peatlands formed in the West Siberian Lowlands, Hudson Bay Lowlands and Western Canada (Figs. 4b and 1). In total, wetland and peatland area increased by nearly 10-fold between the early and mid-Holocene (from 260 × 10^3 km^2 in 11 ka to 2320 × 10^3 km^2 in 5 ka).

After 5 ka, northern peatland expansion continued at a slower rate (Fig. 4a) as the rate of observed peatland initiation decreased (Fig. 2a). In most regions, the formation of new peatlands was generally low, accounting for <30% of present-day peatland area (Fig. 4a). The exception was Central North America, where new peatland formation after 5 ka accounted for more than 40% of the total regional area as peatlands continued to form in the Hudson Bay Lowlands and in the northern boreal parts of Alberta, Manitoba, and Saskatchewan (Figs. 1 and 4b).

The composition of peatlands changed substantially over time. Model results showed that prior to 5 ka, 64% of peatland area was composed of early peatland successional stages: marshes, open-water wetlands and fens (Fig. 4a). After 5 ka, many of these marshes, open-water wetlands and fens transitioned to bogs and permafrost peatlands (Fig. 4a). By 1 ka, the area of marshes, open water wetlands and fens comprised only 45% of total wetland area, while bog and permafrost peatland areas nearly doubled in size (Fig. 4a). Widespread permafrost presence in northern peatlands increased sharply after 1 ka (Fig. 4a) as permafrost formed in Canada, across Siberia, and in Northwest (European) Russia (Fig. 3). We estimate that an additional 670,000 km^2 of peatlands were affected by permafrost after 1 ka, which suggests that approximately two-thirds of permafrost peatlands aggraded permafrost relatively recently.

3.3. Northern peatland and wetland CH_4 emissions during the Holocene

Northern peatland expansion was one of the dominant drivers of increased northern extra-tropical peatland CH_4 emissions during the Holocene (Figs. 4a and 5a). Prior to the Holocene (>11.6 ka), modeled northern peatland and wetland emissions were <6 Tg CH_4 y^{-1} due to the relatively small peatland area. The major source regions were central North America and Alaska (Fig. 5b). The fastest modeled growth in northern wetland CH_4 emissions occurred in the early to mid-Holocene (10.6–6.9 ka) during a period of major wetland formation and expansion across northern high latitudes (Figs. 4a and 5a), when emissions increased from ~8 to 33 Tg CH_4 y^{-1}. The major source regions of CH_4 emissions during this period included West and Central Siberia and Central North America due to the expansion of fens (Fig. 5), which was inferred from basal ages and plant macrofossil records (Figs. 2 and 3). During this period, the majority (64%) of peatland area was composed of high-emitting marshes, open-water wetlands and fens (Fig. 4a, Table 2). Combined, these wetland classes emitted >90% of the total modeled wetland CH_4 emissions (Fig. 5a).

Despite the continued increase in peatland area between 5 ka

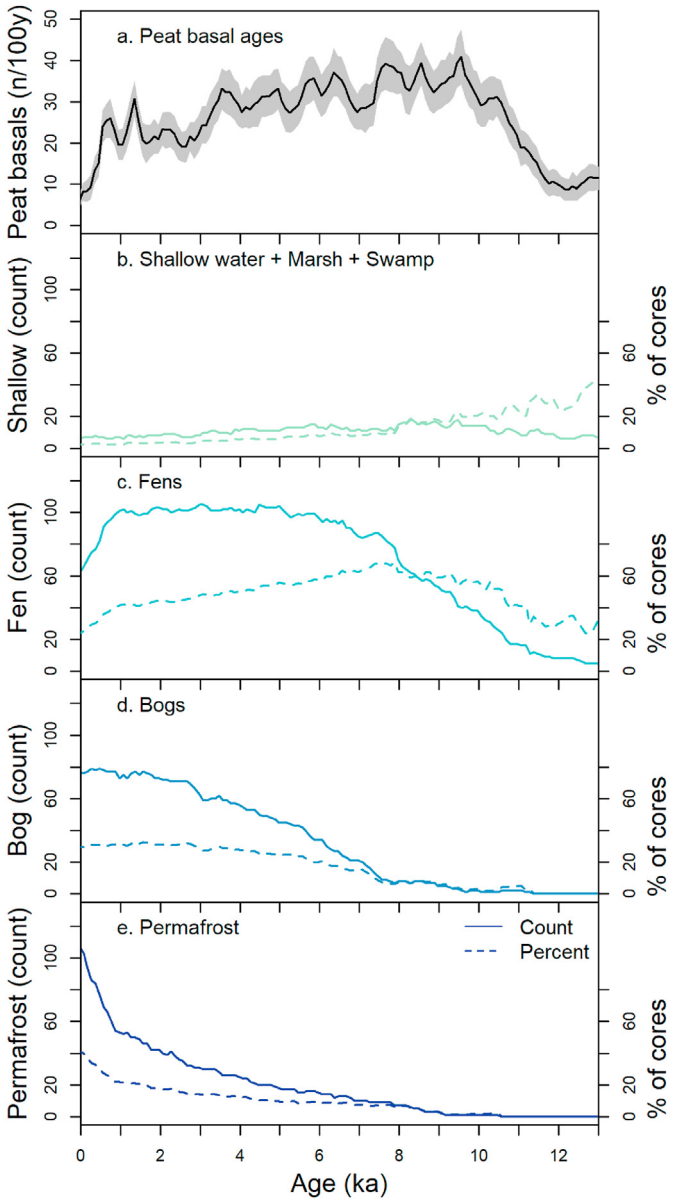

Fig. 2. Time series of peatland initiation rates (panel a, from peat basal ages) and peatland type (panels b–e, from peat core records) as counts (panels b–e; left axis, solid lines) and normalized to the number of cores (right axis, dashed lines). The peatland types of interest were: b) shallow water wetlands, marshes, and swamps; c) fens without permafrost, including rich fens, poor fens, and intermediate fens; d) bogs without permafrost; e) permafrost peatlands, including peat plateaus, polygonal peatlands, and tundra peatlands.

and 1 ka (Fig. 4a), total peatland CH_4 emissions stabilized at 42 ± 26 Tg CH_4 y^{-1} as marshes, open-water wetlands and fens transitioned to lower-emitting bogs and permafrost peatlands (Figs. 5a and 3). By 5 ka, 90% of CH_4 emissions were from mashes, fens, and open water wetlands, while the remainder was from drier bogs and colder permafrost wetlands. By 1 ka, ~80% of emissions were still from marshes, fens, and open water wetlands, despite these classes making up < 50% of the modeled peatland area (Fig. 4a).

While the fen-bog transition played an important role in stabilizing wetland CH_4 emissions as peatlands expanded, the formation of permafrost across northern high latitudes resulted in the strongest net decrease in CH_4 emissions (Figs. 3 and 5a). With the 67% increase in peatland area affected by permafrost after 1 ka (Fig. 4a), modeled northern wetland CH_4 emissions decreased by ~20%–34 ± 26 Tg CH_4 y^{-1} in the present-day (Fig. 5a). As a result, 15% of present-day CH_4 emissions from northern peatlands (~5 Tg y^{-1}) can be attributed to permafrost peatlands.

4. Discussion

4.1. Role of northern extra-tropical peatland emissions in the global CH_4 budget

Our present-day northern peatland CH_4 flux of 34 ± 26 Tg y^{-1} is consistent with but at the low end of other estimates of northern wetland emissions, which range from 31 to 65 Tg y^{-1}, and include both a larger geographic area and non-peatland wetlands and inundated areas (Saunois et al., 2016; Thompson et al., 2017; Treat et al., 2018) depending on the study domain and the sources considered. Our estimate of present-day emissions for Canada, Alaska, and northern parts of the U.S. (Fig. 1) was 13.2 Tg CH_4 y^{-1}, with 2.1 Tg CH_4 y^{-1} from Alaska. These emissions are substantially larger than earlier estimates of growing season wetland emissions of 4.1–6.9 Tg CH_4 $season^{-1}$ for Canada (Webster et al., 2018) and annual emissions of 6.1 Tg CH_4 y^{-1} for Canada and Alaska (Bridgham et al., 2006). These differences in peatland CH_4 emissions from North America between this study and others may be driven by difference in wetland types considered (including the presence/absence of permafrost) and differences in CH_4 flux rates, including differences from sites with and without permafrost and winter CH_4 emissions. Importantly, the modeled areas of bogs, fens, and permafrost peatlands fell within the earlier estimates for Canada (Table 1, Table S2).

Overall, the timing of increases in northern wetland and peatland emissions show little correlation with atmospheric CH_4 records from ice cores (Fig. 6a and b). Using atmospheric box models, northern hemisphere sources were inferred as 155–180 Tg CH_4 y^{-1} during the Holocene (Bock et al., 2017). Against these estimates, CH_4 emissions from extant peatlands were a relatively small component of northern hemisphere CH_4 emissions, and ranged from 5 to 43 Tg CH_4 y^{-1}, or 5–27% of northern hemisphere sources (Fig. 5b and c, Beck et al., 2018). The relatively small magnitude of northern peatland emissions during the Holocene (<45 Tg CH_4 y^{-1}) as well as often opposing trends (Fig. 6b) points toward other regions and/or other sources being the dominant drivers of global and northern hemisphere CH_4 emissions rather than extant northern peatlands. Potential other northern CH_4 sources could include permafrost thaw and thermokarst lakes and wetlands (Brosius et al., 2021), glacial lakes (Brosius et al., 2021), exposed continental shelves (Kaplan, 2002; Kleinen et al., 2020), non-peat forming northern wetlands (Yu et al., 2013; Byun et al., 2021), and/or wildfire (Bock et al., 2017).

However, parsing the magnitude of other northern hemisphere sources is difficult both between latitudinal regions (e.g. tropics vs. northern high latitudes) and among source types due to limitations of paleoclimate and paleoecological proxies. Other studies have indicated that tropical wetlands were likely the dominant driver of global CH_4 emissions during the Holocene (Bock et al., 2017; Rhodes et al., 2017; Singarayer et al., 2011); emissions from tropical wetlands occur in both northern and southern hemispheres. Bottom-up reconstructions and modeling of tropical wetland emissions based on observations of tropical wetland dynamics are limited by an understanding of tropical wetland dynamics and extent even in the present-day but do point to the importance of these regions (Kleinen et al., 2020). Information on past tropical wetland dynamics is even more limited than present-day (Treat et al., 2019).

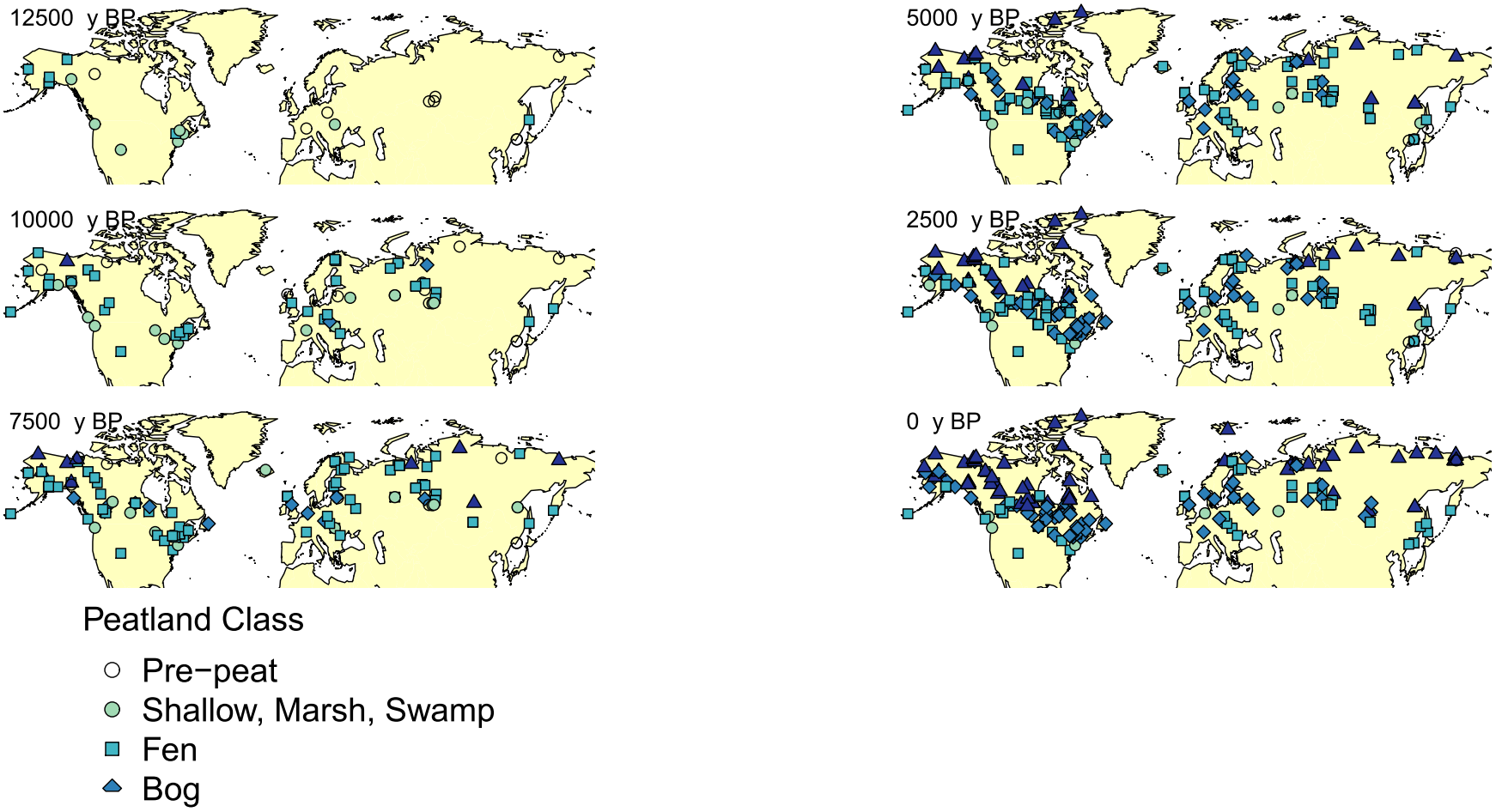

Fig. 3. Maps showing the peatland type indicated by the plant macrofossils in the 262 peatland cores included in the study from 12.5 ka to 0 ka.

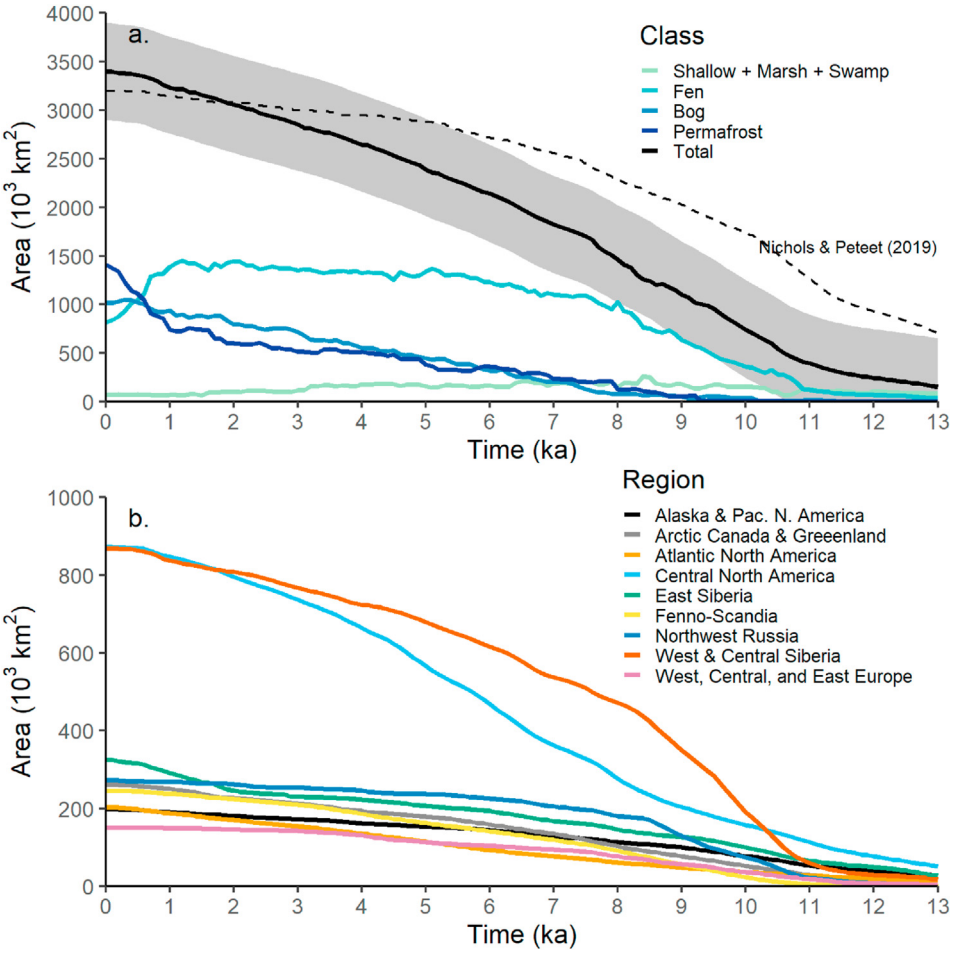

Fig. 4. Reconstructed peatland areas from 13 ka to present by wetland class and region. a) Area by wetland class with total peatland area shown by the black line and uncertainty shown by the gray ribbon; b) Area differentiated by region. Time resolution is 100 years; ka: 1000 years BP. Wetland classes include combined shallow water wetlands, marshes and swamps; fens (including rich, poor, intermediate, and not specified), bogs, and permafrost peatlands (including peat plateaus, polygonal peatlands, and tundra peatlands).

4.2. Peatland and wetland dynamics during the Younger Dryas (13 ka – 11.6 ka)

Several studies hypothesized that the early formation of wetlands and peatlands represented a major new source of CH_4 to the atmosphere, corresponding to the abrupt increase in atmospheric CH_4 at the end of the Younger Dryas (MacDonald et al., 2006; Yu et al., 2013). While Central North America and Alaska were the major source regions for wetland CH_4 emissions during the Younger Dryas (Fig. 5b) because of early peatland formation in the Great Lakes Region and Alaska (Figs. 1 and 3), we found little correlation between the records of atmospheric CH_4 and northern wetland CH_4 emissions using a larger dataset of peatland initiation dates (Fig. 6d). Peatland and pre-peatland wetland CH_4 emissions from extant peatland areas were modeled as 5 ± 5 Tg CH_4 y^{-1} prior to the end of the Younger Dryas and were limited by small wetland area rather than wetland type, as most wetlands were fens and other high-emitting wetland classes (Figs. 4a, 5a and 3). At 12.1 ka, northern peatland emissions represented ~10% of the northern extra-tropical sources of 48 ± 4 Tg CH_4 y^{-1} and 5% of northern hemisphere sources (96 Tg CH_4 y^{-1}) inferred from ice core records (Baumgartner et al., 2012).

Unlike the atmospheric CH_4 concentrations that increased rapidly at the end of the Younger Dryas beginning around 11.7 ka, northern peatland CH_4 emissions increased slowly (Fig. 6a and c). The modeling approach that we used in this study did not capture a rapid peatland response to warming that resulted in large CH_4 emissions. However, there is significant uncertainty in the reconstruction of wetland area and CH_4 flux during the Younger Dryas (Figs. 4a and 5a). If large peatland areas formed earlier and expanded faster than found in this study, as proposed by both Nichols and Peteet (2019) and MacDonald et al. (2006), or were more extensive in the past than in the present-day due to peatland loss and burial (Treat et al., 2019), total wetland emissions could have been substantially larger, as could the rate of increase in peatland CH_4 fluxes at the end of the Younger Dryas. Using the peatland areas proposed by Nichols and Peteet (2019) shown in Fig. 4a for the Younger Dryas and CH_4 flux rates based on the observed peatland types (e.g. Fig. 2), annual peatland CH_4 emissions at 12.1 ka would be five to six times larger than we estimated, ranging from 23 to 32 Tg CH_4 y^{-1}. Nichols and Peteet (2019) also found an increase in peatland area of 275,000 km^2 between the end of the Younger Dryas (11.7 ka) and 11 ka that was two to three times larger than what we found in this study (Fig. 4a), which would have resulted in an increase of northern peatland CH_4 emissions of ~10 Tg CH_4 y^{-1} rather than 3 Tg CH_4 y^{-1} that this study found (Fig. 5a). Still, even a 10 Tg CH_4 y^{-1} increase under the rapid peatland expansion scenario proposed by Nichols and Peteet (2019) is relatively small compared to modeled northern hemisphere sources of ~150 Tg CH_4 y^{-1} or the size of the sources responsible for

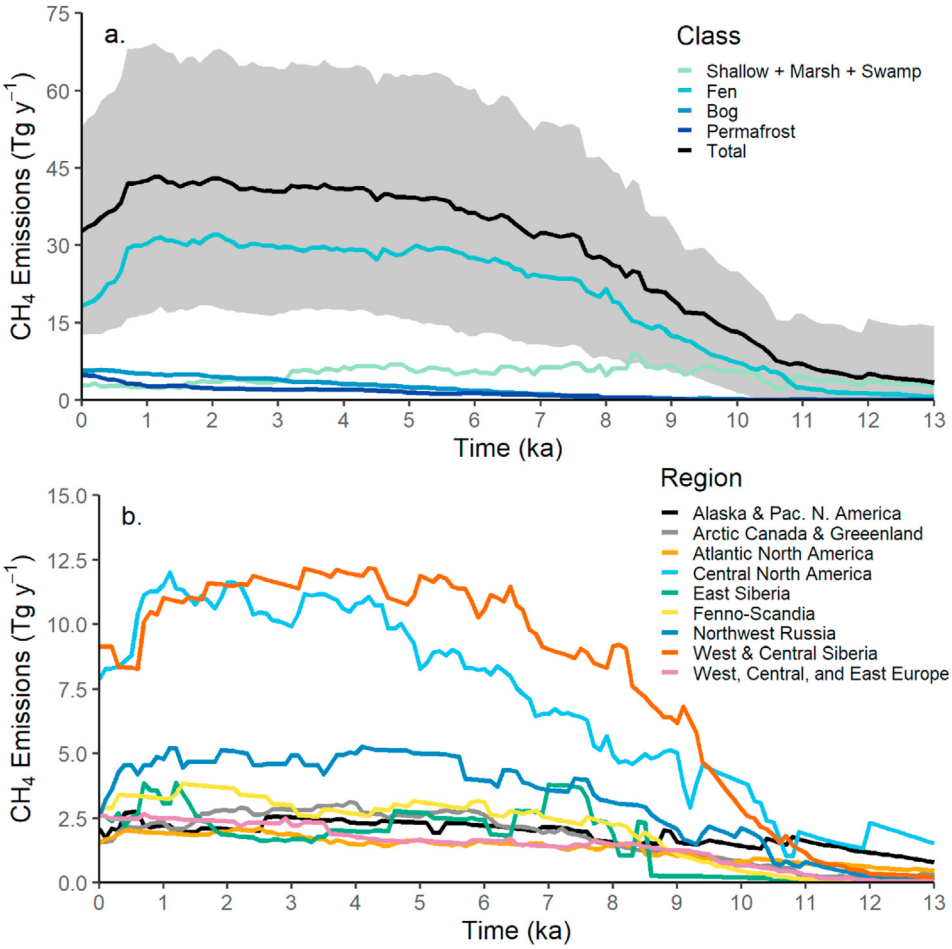

Fig. 5. Reconstructed wetland and peatland CH_4 emissions from 13 ka to present by wetland class and region. a) The contribution of individual wetland classes to the total CH_4 flux from high latitude wetlands with total emissions shown by the black line and uncertainty in total emissions shown by the gray ribbon; b) CH_4 emissions differentiated by region. Time resolution is 100 years; ka: 1000 years BP. Wetland classes include combined shallow water wetlands, marshes and swamps; fens (including rich, poor, intermediate, and unspecified), bogs, and permafrost peatlands (including peat plateaus, polygonal peatlands, and tundra peatlands).

the rapid increase of atmospheric CH_4 (Fig. 6b, Beck et al., 2018). From this, it is likely that the rapid formation of northern peatlands and subsequent CH_4 emissions were at most a relatively minor driver of the rapid increase in atmospheric CH_4 concentrations at the end of the Younger Dryas (Fig. 6a).

4.3. Early Holocene (10–8 ka): rapid wetland expansion

By 10 ka, extant peatland areas more than doubled from the Younger Dryas (Fig. 4a), but the increased peatland CH_4 flux comprised a similar percentage (~10%) of total northern hemisphere CH_4 emissions because these emissions also increased (Fig. 6c). Previous studies of atmospheric CH_4 have invoked widespread fen-to-bog transitions during this period in order to explain changes of $\delta^{13}C$ in atmospheric CH_4 (Beck et al., 2018; MacDonald et al., 2006). However, we find little evidence for widespread fen-to-bog transitions in extant peatlands before 7.5 ka using paleoecological records from peatlands (Fig. 3). Instead, these transitions predominately occur after 7.5 ka (Figs. 2 and 3).

While this reconstruction found that northern peatlands contributed ~10% of the 175 Tg CH_4 y^{-1} northern hemisphere sources at 10 ka (Fig. 5c; Beck et al., 2018), using different methods to estimate peatland and wetland area produced substantially different results. For example, a recent process-based modeling study found that the contribution of northern extra-tropical inundated sources was substantially larger: 48 Tg CH_4 y^{-1}, or ~30% of the northern hemisphere sources (Kleinen et al., 2020). The areal CH_4 flux rate from Kleinen et al. (2020) was about 20% lower compared to this study, so differences were due to the larger source area, which included lakes and ponds as well as other source areas like terrestrial wetlands on shelf areas in Beringia that flooded with deglacial sea level rise (Kleinen et al., 2020; Treat et al., 2019). A recent synthesis of northern lake basal ages found that lake formation occurred earlier than peatland formation (Brosius et al., 2021), which would support a larger northern source region that occurred earlier in addition to peatlands. Using the larger peatland areas at 10 ka from Nichols and Peteet (2019) and flux rates from this study, peatland emissions were 44 Tg CH_4 y^{-1}, similar to Kleinen et al. (2020).

4.4. Mid-Holocene (8–5.5 ka): fen to bog transitions

Peatland expansion continued during the mid-Holocene and northern wetland CH_4 emissions rose from 28 ± 19 to 40 ± 26 Tg CH_4 y^{-1} (Fig. 5a), which increased their contribution from <20% to >25% of northern hemisphere emissions (Fig. 6c). Increased peatland CH_4 emissions between 8 ka and 5.5 ka were mainly driven by large areas of fen formation, particularly in central North America, as well as continued peatland expansion in West and Central Siberia (Figs. 3, 4a and 5b). Despite the increase in reconstructed

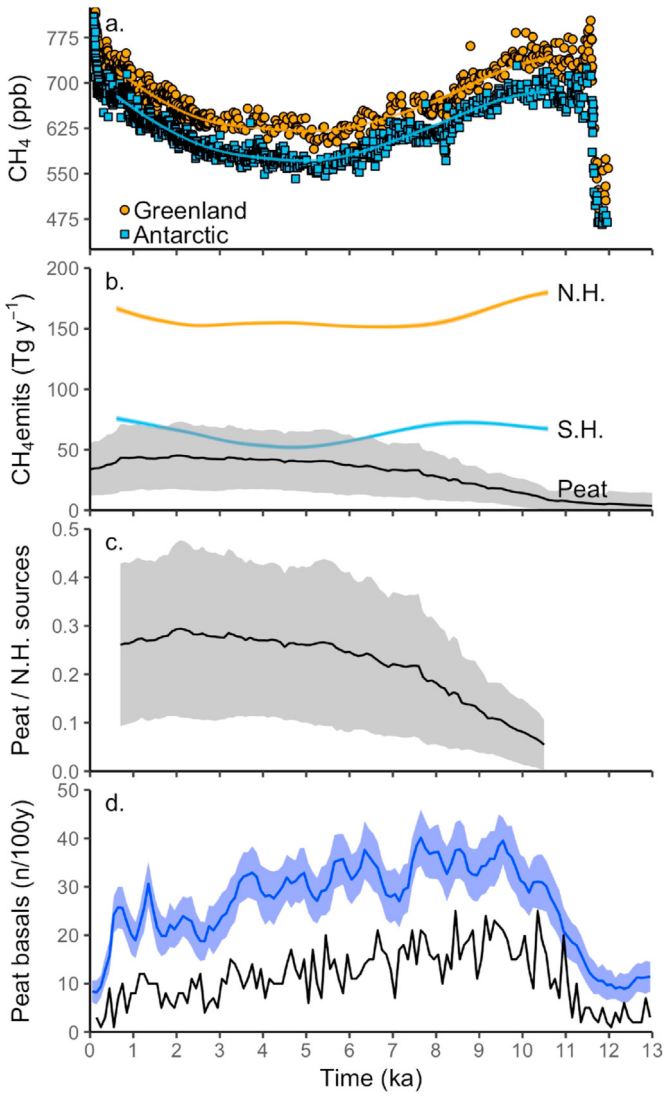

Fig. 6. Time series comparing atmospheric CH_4, inferred CH_4 emissions, and northern peatland emissions. a) ice core records of CH_4 concentrations from Greenland (orange) and Antarctica (blue; Beck et al., 2018); b) inferred CH_4 emissions from top-down models of northern hemisphere (N.H., orange) and southern hemisphere (S.H., blue) sources excluding uncertainty due to the atmospheric lifetimes of CH_4 (Beck et al., 2018), and CH_4 emissions from extant northern peatland (Peat, gray, this study); c) the fractional contribution of peatlands to inferred northern hemisphere sources (again, excluding uncertainty due to atmospheric life time; Beck et al., 2018); d) frequency of peatland basal ages per century used in the study (blue line, blue bands) and from MacDonald et al. (2006; black line). The shaded bands represent error due to uncertainty from areas and flux rates (b and c) and in radiocarbon ages (d). (For interpretation of the references to color in this figure legend, the reader is referred to the Web version of this article.)

northern wetland and peatland CH_4 emissions during this period, the total inferred northern hemisphere CH_4 emissions remained relatively stable (Fig. 5b; Beck et al., 2018), again suggesting that northern peatlands were not the major driver of global or northern wetland emissions. The stable northern hemisphere emissions despite increases in northern peatland emissions implies a decrease in other northern hemisphere CH_4 sources between 8 ka to 5.5 ka to offset these reconstructed northern peatland emissions. If southern hemisphere tropical wetland emissions decreased during this period as suggested by others (Beck et al., 2018; Singarayer et al., 2011), decreased emissions from tropical wetlands in the northern hemisphere is also possible. While total northern hemisphere CH_4 emissions may have changed little between 8 ka and 5.5 ka, the fraction of emissions from the tropics vs. northern high latitudes likely shifted during this period to accommodate the increased northern peatland emissions (Fig. 6c).

4.5. Late Holocene to present day (5.5 ka − present): permafrost formation

Peatland emissions were nearly stable during the late Holocene despite continued wetland expansion due to internal successional processes, namely the fen to bog transitions but also permafrost aggradation, which both reduced areal CH_4 flux rates (Table 2). During this period, rates of peatland initiation decreased (Fig. 2a); earlier studies showed that northern peatland expansion during this period occurred mainly via paludification, also referred to as lateral expansion across the landscape (Korhola et al., 2010; Ruppel et al., 2013). This method of peatland expansion does not generally lead to the formation of high-emitting early successional peatland stages (such as shallow-water wetlands, marshes, and swamps), which is reflected in the small number of these records during this period (Figs. 2b and 3). The continued transition of fens to bogs was very apparent, particularly in North America, but even more notable was the widespread aggradation of permafrost in peatlands (both fens and bogs) between 5 ka and present-day (Fig. 3).

While the fen-bog transition played an important role in stabilizing wetland CH_4 emissions as peatlands expanded, the formation of permafrost in peatlands across northern high latitudes resulted in a strong net decrease in CH_4 emissions of ~20%–34 ± 21 Tg y^{-1} in the present-day (Fig. 5a). The decrease in peatland emissions during the last thousand years again showed no correlation with atmospheric CH_4 concentrations in the ice core record (Fig. 6) and likely reflects the importance of other CH_4 sources in the global budget during the late Holocene (Mitchell et al., 2013). Northern peatland emissions comprised ~25% of northern hemisphere emissions at both 5.5 ka and 1 ka, coinciding with increasing northern hemisphere emissions (Fig. 6). During this period, areal estimates of peatland extent from this study agreed better with other areal estimates using different approaches, resulting in estimated northern wetland and peatland emissions of 43–58 Tg CH_4 y^{-1} (Fig. 4a; Kleinen et al., 2020; Nichols and Peteet, 2019).

The extensive permafrost formation in peatlands during the last thousand years under regionally colder climates (Figs. 3 and 4a) implies an enhanced vulnerability to permafrost thaw as climate warms and if ecosystem protections (e.g. moss layers) are disturbed (Halsey et al., 1995; Shur and Jorgenson, 2007). Given the vulnerability of much of extensive regions of permafrost peatlands, there is a strong likelihood of higher CH_4 emissions as permafrost thaws (e.g. Hugelius et al., 2020) and CH_4 flux rates return to similar rates to before permafrost formed. Permafrost thaw in peatlands largely results in an inundation of the peat surface and a roughly sevenfold increase in CH_4 flux (Table 2), which could increase annual CH_4 flux from boreal zone peatlands by as much as 2 to 14 Tg y^{-1}, if peatlands became drier (bogs) or wetter (fens, newly thawed permafrost), respectively.

4.6. Opportunities for improving quantification of northern wetland and peatland CH_4 flux during the Holocene

4.6.1. Methane fluxes

One major limitation of this empirical modeling approach to the reconstruction of wetland CH_4 flux is the issue of non-analogous CH_4 fluxes, i.e., that present-day flux measurements may not be representative of past fluxes. Methane flux rates are the net result of production, oxidation, and transport, which have different controlling factors but can simplified to temperature (controls rates of

microbial processes), water table (controls the balance between zones of anaerobic production and aerobic consumption), and vegetation composition and productivity (controls transport via aerenchymous plants as well as amount of substrate) (Bridgham et al., 2013). Vegetation composition is constrained by the macrofossil assemblages and given the range of water table conditions wetland plants associated with the different wetland types are, these parameters are likely relatively well constrained. However, changing insolation during the Holocene impacted growing season temperatures and length, which is harder to constrain by our reconstruction. High summer insolation in the early Holocene resulted in warmer-than-present conditions in many peat-forming regions in the northern high latitudes (Kaufman et al., 2004; MacDonald et al., 2006; Jones and Yu, 2010), likely impacting CH_4 production, but it is unclear how their magnitudes compared with today.

Higher CH_4 flux rates in the past, particularly during the early Holocene, have been proposed as a result of warmer growing season temperatures corresponding to higher apparent vegetation productivity (Yu et al., 2013) and many peatlands exhibit high rates of carbon accumulation in their early stages and in the early Holocene (Jones and Yu, 2010; Loisel et al., 2014). Our model shows that the mean areal CH_4 flux rate was three times higher in 11.6 ka than today due to the predominance of high-emitting fens, marshes, and open water wetlands, while today more than 50% of the peatland area is composed of low-emitting bogs and permafrost peatlands (Fig. 4a). However, the few process-based modeling studies to calculate wetland CH_4 emissions over these long time periods found *lower* CH_4 flux rates in the late glacial and early Holocene than the present due to the effects of CO_2 fertilization and warm summer (and winter) temperatures today (Kaplan, 2002; Kleinen et al., 2020). While a process-based model is an ideal tool to explore the net effects of longer growing seasons, warmer summer temperatures, and wetter conditions on CH_4 flux rates, significant uncertainty remains in the parameterization due to limited data about the processes underlying CH_4 fluxes: production, oxidation, and transport, even in the present day (Xu et al., 2016). Furthermore, process-based models are generalized across vegetation types, while CH_4 flux rates differ significantly among vegetation types (Bubier, 1995) and subsequently, among wetland classes (Table 2). This study demonstrates the importance of considering and differentiating between wetland types (Fig. 5a). A modeling approach that can capture the differences in CH_4 flux between fens, bogs, and permafrost peatlands as well as model the response of fluxes to insolation, seasonal temperature differences, and CO_2 fertilization would be the ideal way to move forward.

Our estimate of northern peatland CH_4 flux was particularly sensitive to the annual CH_4 flux from fens given their large area during the Holocene (Fig. 4a). This was demonstrated with a simple sensitivity analysis using annual fluxes estimated from growing season measurements rather than annual measurements and the area measurements from Fig. 4 (Table S3; Treat et al., 2018). While annual emissions from bogs decreased by <5% with the inclusion of nearly 90 additional measurements, annual CH_4 emissions from fens were 50–65% smaller except in rich fens (Table S3). Using these smaller CH_4 fluxes from fens resulted in substantially smaller peatland emissions (20%) throughout the Holocene and in the present day, although emissions still fell within the original range of uncertainty (Figure S1). Annual emissions were 6.8 Tg CH_4 y^{-1} (20%) lower overall, and emissions from central North America (the major driver of Canadian emissions) were estimated at 6.7 Tg CH_4 y^{-1}, closer to emissions from Webster et al. (2018) for Canada. This points to the relatively high uncertainty and high spatial variability of annual CH_4 flux measurements from fens, which might not be surprising given the broad range of vegetation, hydrology, and geochemistry encompassed by this peatland class. That the results using different CH_4 fluxes still fell within the original range of uncertainty in northern peatland CH_4 emissions (Figure S1) also demonstrates that the statistical approach to representing uncertainty in CH_4 fluxes that we used adequately captures this variability.

Methane fluxes may have also differed in the past due to different water tables and vegetation composition. For example, European peatlands are drier today than during the past 1000 years (Swindles et al., 2019), which might bias the present-day measurements of CH_4 flux that we use in the reconstruction towards smaller fluxes (e.g. Blodau, 2002) and could mean that past emissions were larger than found in this study. Similarly, it is possible that the wetland classification used to model CH_4 fluxes based on present-day vegetation communities may not directly translate to past vegetation communities and wetland types based on macrofossil assemblages (Byun et al., 2021). Preservation of individual species varies through time and among sites, and inferences must be made on broader categories of peat composition (i.e., bryophytic, herbaceous, ligneous). However, the approach used in this study does account for the presence of sedges, which are correlated with larger CH_4 emissions in northern wetlands (Bubier, 1995; Treat et al., 2018), are indicative of wet conditions, and are evident in the macrofossil records (Charman, 2002; Treat et al., 2016), likely giving a solid first-order estimate of northern wetland CH_4 flux. Difficulties also emerge when vegetation communities and plant macrofossils between wetland classes are similar, such as with some bogs and permafrost plateaus (Treat et al., 2016), although both have relatively low CH_4 flux rates (Table 2).

4.6.2. Wetland and peatland areas

We compared our results to two other recent studies, peatland areas to Nichols and Peteet (2019), where we also used their area reconstruction to compute CH_4 emissions, and CH_4 emissions and components (CH_4 flux rates and wetland areas to Kleinen et al. (2020)), in order to better constrain the uncertainty in the reconstructed CH_4 emissions from this study. Nichols and Peteet (2019) reconstructed northern peatland areas for a slightly larger high latitude region (study domain extended further south) using a statistical approach based on the cumulative basal ages and including additional basal ages from the U.S. Midwest. They found more peatland initiation earlier than in this study (Fig. 4a, dashed line). Using the larger areas in the early Holocene from Nichols and Peteet (2019) increased total CH_4 emissions substantially, five to six times larger than we estimated during the Younger Dryas, but peatland emissions were still not the dominant contributor to total northern hemisphere emissions (43–58 Tg CH_4 y^{-1} vs. > 150 Tg CH_4 y^{-1} emissions from Beck et al., 2018).

Overall, the disadvantage to basing past wetland areas on present-day peatland areas and cumulative basal ages is that this approach underestimates the past CH_4-producing wetland area to some extent. Some areas that were wetlands and peatlands during the Holocene are not found in the present day, including formerly exposed continental shelves and regions that were drained for agriculture (Treat et al., 2019; Byun et al., 2021). Using wetland areas from process-based modelling that captured climate, topography, and reconstructed sea levels, Kleinen et al. (2020) modeled dynamic wetland areas over time, including wetlands formed on now-inundated coastal shelves. They found that larger northern wetland emissions during the early Holocene (10 ka) due to a larger source area but lower CH_4 emission rates than in this study; this trend held to the pre-industrial period. It is unclear how much of this larger source area was due to peatlands; the wetland areas they used were based on satellite-derived inundation maps and can include lakes and ponds. Lakes and ponds can produce CH_4 but are

not wetlands and have poorly quantified emissions (Wik et al., 2016); their areas were also dynamic during the Holocene (Brosius et al., 2021). In addition, some wetland areas are missed by satellite classifications of inundation because they have trees (Webster et al., 2018) or the water table is below the soil surface (Minasny et al., 2019), either because wetlands are only seasonally rather than permanently inundated or because thick organic soils obscure the easy detection of saturated soil, as occurs in peatlands.

One major limitation for model validation of CH_4 emissions is the maps of methane-emitting areas, including the separation of permanent wetlands, peatlands, seasonally inundated wetlands, lakes, rivers, and ponds and within peatland types. Recent advances using remote sensing may help to tease out these important, yet different, sources of CH_4 (Matthews et al., 2020), although some issues remain, like the absence of peatlands in Arctic Canada (Webster et al., 2018). For peatlands and wetlands, further classification data like the proportion of fens and bogs or vegetation species composition are needed across northern high latitudes in order to determine whether disagreements in total CH_4 flux between process-based models and other observations are due to problems in the modeled CH_4 flux rates or in the areal inputs (Melton et al., 2013).

In northern latitudes, non-peat-forming seasonally or permanently flooded wetlands comprise an additional and potentially important CH_4 emissions source (Bridgham et al., 2006; Treat et al., 2018). Our approach to reconstructing areas misses those additional sources that are not present on the landscape today, which could have occurred in large wetland areas that either did not form peat, and are excluded from our analysis, or formed peat (basal dates) much later, and so arrive late in our analysis (e.g. "pre-peatland wetlands" in Alaska; Yu et al., 2013). While we include some of these wetland areas (marshes) if they later formed peat (Fig. 4), this is likely an underestimation of total methane-producing wetland area, which could shift the wetland areas closer to those found in the other studies (e.g. Kleinen et al., 2020; Nichols and Peteet, 2019). Additionally, other wetlands not on the landscape today (e.g. buried peat) are not explicitly included in these CH_4 emissions estimates because of limited information on location and extent, but are implicitly included in the flux error given the relatively large area uncertainty used in the analysis (Fig. 4). This includes peatlands that were buried or otherwise lost from the landscape (Treat et al., 2019), like in Beringia, which would have been an additional CH_4 source in the early Holocene and LGM. Peatland area was also lost due to peat mining and artificial drainage, which has occurred during the 19th and 20th centuries in large areas of the American Midwest (Byun et al., 2021; Prince, 1998) and Europe (Joosten and Clarke, 2002) including relatively large areas in Ireland, Scotland, Germany and Poland. In these cases, while we have some idea of the locations, an understanding of the extent of these wetlands is lacking and would benefit future estimates. This is a basic requirement before these regions can be accounted for in past CH_4 budgets. Finally, additional sampling from understudied regions, particularly in central and eastern Siberia (Table 1), in order to determine both CH_4 flux rates and the ecosystem development history, would be useful to further refine these first continuous estimates of northern peatland CH_4 flux.

4.6.3. Reconciling top-down and bottom-up comparisons of atmospheric CH_4 budgets

Atmospheric box modeling is a useful tool to separate tropical northern hemisphere emissions from northern high-latitude CH_4 sources (Bock et al., 2017), but it does encounter some limitations. Modeling to quantify the impact of differences in atmospheric lifetimes of CH_4 over time resulted in emissions differences of as much as 10% (Hopcroft et al., 2018; Murray et al., 2014), which changes the relative fraction of northern peatland emissions, but does not change the disagreement between the records or that northern peatlands are a relatively small component of total emissions. Recent analysis has shown the presence of dust in ice cores from Greenland can cause artefacts in the CH_4 record (Lee et al., 2020); quantifying the impact of this finding on the Holocene CH_4 record will require additional analyses and sampling. Additional proxies like radiocarbon and isotopic measurements have been used to separate some old-carbon sources of CH_4 (e.g. gas hydrates and permafrost thaw) from contemporary biogenic production (Dyonisius et al., 2020); further creative approaches may be required to partition emissions among wetlands (including tropical and northern) and other high-latitude northern sources using these top-down approaches and constraints.

Despite the relatively large uncertainties in northern peatland CH_4 emissions in this study (Fig. 5b), these results still provide important insights into northern CH_4 budgets for the last 13 ka. We show important differences from top-down model inferences, including observations of the later timing of fen-bog transitions and the importance of permafrost aggradation to CH_4 fluxes. While emissions are not insignificant, without substantially larger area and/or CH_4 fluxes, extant northern peatlands do not appear to be the dominant driver of atmospheric CH_4 concentrations either during the Younger Dryas or during the Holocene (Fig. 6). A recent synthesis of lake CH_4 emissions during the Holocene shows that peak initiation rates from lakes precede peak northern peatland emissions but were likely of a similar or smaller magnitude (Brosius et al., 2021). Similar bottom-up approaches across other known and hypothesized sources (e.g. thermokarst lakes, non-peat forming wetlands, exposed continental shelves, tropical wetlands, wildfire) would also be a useful complement to top-down approaches by providing first-order estimates of emissions utilizing the observational constraints. More observations of tropical wetlands, including improved area estimates, understanding of temporal dynamics, and CH_4 estimates in the present day are also key to resolving past emissions.

5. Conclusions

The results of this study show that CH_4 emissions during the Holocene from extant northern peatland are nearly completely decoupled from trends in atmospheric CH_4 concentrations and modeled northern hemisphere CH_4 emissions using top-down approaches, even after accounting for fen-bog transitions, permafrost aggradation, and CH_4 flux rate differences among wetland types. These results suggest that other sources were likely the major drivers of atmospheric CH_4 at the end of the Younger Dryas and throughout the Holocene. While peatland CH_4 emissions from present-day peatland areas accounted for 20–25% of total northern hemisphere emissions during the past 5 ka (Fig. 6c), we found that the role of extant peatlands in the early Holocene was likely limited by their small spatial extent. How peatland area developed over time remains the largest factor of uncertainty in these reconstructions, with wide variation among different estimates for areas before 5 ka. Permafrost aggradation and ecosystem succession (from marshes and shallow water wetlands to fens and then bogs) in peatlands have significantly limited the increase in CH_4 emissions throughout the Holocene than would have been expected from wetland expansion alone. The past peatland areas modeled using this reconstruction method will likely require revision in the future with additional evidence for earlier (or later) peatland formation as new peatland basal ages are published and compiled or new peatland areas are mapped in poorly known regions (e.g. Eastern Siberia, Fig. 1). Further efforts to reconcile atmospheric records of CH_4 concentrations and isotopes with

empirical and process-based models are necessary, but consideration of differences among northern wetland types is critical, particularly associated with permafrost formation.

Author statement

Claire C. Treat: Conceptualization, Data curation, Formal analysis, Funding acquisition, Methodology, Validation, Writing – original draft, Writing – review & editing Miriam C. Jones: Conceptualization, Formal analysis, Funding acquisition, Methodology, Supervision, Writing – original draft, Writing – review & editing Laura Brosius: Conceptualization, Funding acquisition, Methodology, Writing – original draft. Guido Grosse: Conceptualization, Formal analysis, Funding acquisition, Methodology, Visualization, Writing – original draft, Writing – review & editing. Katey Walter Anthony: Conceptualization, Data curation, Funding acquisition, Methodology, Project administration, Writing – original draft, Writing – review & editing. Steve Frolking: Formal analysis, Project administration, Supervision, Writing – original draft, Writing – review & editing.

Declaration of competing interest

The authors have no competing interests to declare.

Acknowledgements

We thank G. Hugelius for data contributions, T. Laepple and T. Sowers for comments on earlier drafts. This project was funded by NSF P2C2 (ARC-1304823, ARC-1903623). CT was supported by European Research Council (#851181) and the Helmholtz Impulse and Networking Fund. MJ is funded by the Climate and Land-use Change Research and Development Program at the USGS. GG was supported by ERC #338335 and BMBF KoPf (#03F0765b).

Appendix A. Supplementary data

Supplementary data to this article can be found online at https://doi.org/10.1016/j.quascirev.2021.106864.

References

Baumgartner, M., Schilt, A., Eicher, O., Schmitt, J., Schwander, J., Spahni, R., Fischer, H., Stocker, T., 2012. High-resolution interpolar difference of atmospheric methane around the Last Glacial Maximum. Biogeosciences 9, 3961–3977.

Beck, J., Bock, M., Schmitt, J., Seth, B., Blunier, T., Fischer, H., 2018. Bipolar carbon and hydrogen isotope constraints on the Holocene methane budget. Biogeosciences 15, 7155–7175.

Blaauw, M., Christen, J.A., 2011. Flexible paleoclimate age-depth models using an autoregressive gamma process. Bayesian Analysis 6, 457–474.

Blodau, C., 2002. Carbon cycling in peatlands- A review of processes and controls. Environ. Rev. 10, 111–134.

Blunier, T., Chappellaz, J., Schwander, J., Stauffer, B., Raynaud, D., 1995. Variations in atmospheric methane concentration during the Holocene epoch. Nature 374, 46–49.

Bock, M., Schmitt, J., Beck, J., Seth, B., Chappellaz, J., Fischer, H., 2017. Glacial/interglacial wetland, biomass burning, and geologic methane emissions constrained by dual stable isotopic CH_4 ice core records. Proc. Natl. Acad. Sci. Unit. States Am. 114, E5778–E5786.

Bridgham, S.D., Cadillo-Quiroz, H., Keller, J.K., Zhuang, Q., 2013. Methane emissions from wetlands: biogeochemical, microbial, and modeling perspectives from local to global scales. Global Change Biol. 19, 1325–1346.

Bridgham, S.D., Megonigal, J.P., Keller, J.K., Bliss, N.B., Trettin, C., 2006. The carbon balance of North American wetlands. Wetlands 26, 889–916.

Brook, E.J., Harder, S., Severinghaus, J., Steig, E.J., Sucher, C.M., 2000. On the origin and timing of rapid changes in atmospheric methane during the Last Glacial Period. Global Biogeochem. Cycles 14, 559–572.

Brosius, L.S., Walter Anthony, K., Treat, C.C., Lenz, J., Jones, M.C., Bret-Harte, M.S., Grosse, G., 2021. Spatiotemporal patterns of northern lake formation since the Last Glacial Maximum. Quat. Sci. Rev. 253, 106773 https://doi.org/10.1016/j.quascirev.2020.106773.

Bubier, J.L., 1995. The relationship of vegetation to methane emission and hydrochemical gradients in northern peatlands. J. Ecol. 83, 403–420.

Byun, E., Sato, H., Cowling, S.A., Finkelstein, S.A., 2021. Extensive wetland development in mid-latitude North America during the Bølling–Allerød. Nat. Geosci. 14, 30–35.

Chadburn, S.E., Aalto, T., Aurela, M., Baldocchi, D., Biasi, C., Boike, J., Burke, E.J., Comyn-Platt, E., Dolman, A.J., Duran-Rojas, C., Fan, Y., Friborg, T., Gao, Y., Gedney, N., Göckede, M., Hayman, G.D., Holl, D., Hugelius, G., Kutzbach, L., Lee, H., Lohila, A., Parmentier, F.-J.W., Sachs, T., Shurpali, N.J., Westermann, S., 2020. Modeled microbial dynamics explain the apparent temperature sensitivity of wetland methane emissions. Global Biogeochem. Cycles 34, e2020GB006678.

Charman, D.J., 2002. Peatlands and Environmental Change. John Wiley & Sons, Chichester, UK.

Dyonisius, M.N., Petrenko, V.V., Smith, A.M., Hua, Q., Yang, B., Schmitt, J., Beck, J., Seth, B., Bock, M., Hmiel, B., Vimont, I., Menking, J.A., Shackleton, S.A., Baggenstos, D., Bauska, T.K., Rhodes, R.H., Sperlich, P., Beaudette, R., Harth, C., Kalk, M., Brook, E.J., Fischer, H., Severinghaus, J.P., Weiss, R.F., 2020. Old carbon reservoirs were not important in the deglacial methane budget. Science 367, 907.

Frolking, S., Talbot, J., Jones, M.C., Treat, C.C., Kauffman, J.B., Tuittila, E.-S., Roulet, N., 2011. Peatlands in the Earth's 21st century climate systems. Environ. Rev. 19, 371–396.

Gorham, E., Lehman, C., Dyke, A., Janssens, J., Dyke, L., 2007. Temporal and spatial aspects of peatland initiation following deglaciation in North America. Quat. Sci. Rev. 26, 300–311.

Halsey, L.A., Vitt, D.H., Zoltai, S.C., 1995. Disequilibrium response of permafrost in boreal continental western Canada to climate-change. Climatic Change 30, 57–73.

Hopcroft, P.O., Valdes, P.J., Kaplan, J.O., 2018. Bayesian analysis of the glacial-interglacial methane increase constrained by stable isotopes and earth system modeling. Geophys. Res. Lett. 45, 3653–3663.

Hornibrook, E., 2009. The stable carbon isotope composition of methane produced and emitted from northern peatlands. In: Baird, A., Belyea, L.R., Comas, X., Reeve, A., Slater, L. (Eds.), Carbon Cycling in Northern Peatlands, pp. 187–203.

Hugelius, G., Loisel, J., Chadburn, S., Jackson, R.B., Jones, M., MacDonald, G., Marushchak, M., Olefeldt, D., Packalen, M., Siewert, M.B., Treat, C., Turetsky, M., Voigt, C., Yu, Z., 2020. Large stocks of peatland carbon and nitrogen are vulnerable to permafrost thaw. In: Proceedings of the National Academy of Sciences, p. 201916387.

Jones, M.C., Yu, Z., 2010. Rapid deglacial and early Holocene expansion of peatlands in Alaska. Proc. Natl. Acad. Sci. Unit. States Am. 107, 7347–7352.

Joosten, H., Clarke, D., 2002. Wise Use of Mires and Peatlands. International mire conservation group, ISBN 951-97744-8-3, p. 304.

Kaplan, J.O., 2002. Wetlands at the last glacial maximum: distribution and methane emissions. Geophys. Res. Lett. 29, 3-1-3-4.

Kaufman, D.S, Ager, T.A, Anderson, N.J, Anderson, N.J, Andrews, J.T, Bartlein, P.J, Brubaker, L.B, Coats, L.L., Cwynar, L.C., Duvall, M.L, Dyke, A.S, Edwards, M.E, Eisner, W.R, Gajewski, K, Geirsdóttir, A, Hu, F.S, Jennings, A.E, Kaplan, M.R, Kerwin, M.W, Lozhkin, A.V, MacDonald, G.M, Miller, G.H, Mock, C.J, Oswald, W.W, Otto-Bliesner, B.L, Porinchu, D.F, Rühland, K, Smol, J.P, Steig, E.J, Wolfe, B.B, 2004. Holocene thermal maximum in the western Arctic (0–180°W). Quat. Sci. Rev. 23 (5-6), 529–560. https://doi.org/10.1016/j.quascirev.2003.09.007. ISSN 0277-3791. https://www.sciencedirect.com/science/article/pii/S0277379103002956.

Kleinen, T., Mikolajewicz, U., Brovkin, V., 2020. Terrestrial methane emissions from Last Glacial Maximum to the preindustrial period. Clim. Past 16, 575–595.

Korhola, A., Ruppel, M., Seppä, H., Väliranta, M., Virtanen, T., Weckström, J., 2010. The importance of northern peatland expansion to the late-Holocene rise of atmospheric methane. Quat. Sci. Rev. 29, 611–617.

Kuhry, P., Halsey, L.A., Bayley, S.E., Vitt, D.H., 1992. Peatland development in relation to Holocene climatic-change in Manitoba and saskatchewan (Canada). Can. J. Earth Sci. 29, 1070–1090.

Lee, J.E., Edwards, J.S., Schmitt, J., Fischer, H., Bock, M., Brook, E.J., 2020. Excess methane in Greenland ice cores associated with high dust concentrations. Geochem. Cosmochim. Acta 270, 409–430.

Lindgren, A., Hugelius, G., Kuhry, P., Christensen, T.R., Vandenberghe, J., 2015. GIS-based maps and area estimates of northern hemisphere permafrost extent during the last glacial maximum. Permafr. Periglac. Process. 27, 6–16.

Loisel, J., Yu, Z., Beilman, D.W., Camill, P., Alm, J., Amesbury, M.J., Anderson, D., Andersson, S., Bochicchio, C., Barber, K., Belyea, L.R., Bunbury, J., Chambers, F.M., Charman, D.J., De Vleeschouwer, F., Fiałkiewicz-Kozieł, B., Finkelstein, S.A., Gałka, M., Garneau, M., Hammarlund, D., Hinchcliffe, W., Holmquist, J., Hughes, P., Jones, M.C., Klein, E.S., Kokfelt, U., Korhola, A., Kuhry, P., Lamarre, A., Lamentowicz, M., Large, D., Lavoie, M., MacDonald, G., Magnan, G., Mäkilä, M., Mallon, G., Mathijssen, P., Mauquoy, D., McCarroll, J., Moore, T.R., Nichols, J., O'Reilly, B., Oksanen, P., Packalen, M., Peteet, D., Richard, P.J., Robinson, S., Ronkainen, T., Rundgren, M., Sannel, A.B.K., Tarnocai, C., Thom, T., Tuittila, E.-S., Turetsky, M., Väliranta, M., van der Linden, M., van Geel, B., van Bellen, S., Vitt, D., Zhao, Y., Zhou, W., 2014. A database and synthesis of northern peatland soil properties and Holocene carbon and nitrogen accumulation. Holocene 24, 1028–1042.

MacDonald, G.M., Beilman, D.W., Kremenetski, K.V., Sheng, Y.W., Smith, L.C., Velichko, A.A., 2006. Rapid early development of circumarctic peatlands and atmospheric CH4 and CO2 variations. Science 314, 285–288.

Mathijssen, P.J.H., Väliranta, M., Korrensalo, A., Alekseychik, P., Vesala, T., Rinne, J., Tuittila, E.-S., 2016. Reconstruction of Holocene carbon dynamics in a large boreal peatland complex, southern Finland. Quat. Sci. Rev. 142, 1–15.
Matthews, E., Johnson, M.S., Genovese, V., Du, J., Bastviken, D., 2020. Methane emission from high latitude lakes: methane-centric lake classification and satellite-driven annual cycle of emissions. Sci. Rep. 10, 9.
Mauquoy, D., Hughes, P.D.M., van Geel, B., 2010. A protocol for plant macrofossil analysis of peat deposits. Mires Peat 7, 1–5.
Melton, J.R., Wania, R., Hodson, E.L., Poulter, B., Ringeval, B., Spahni, R., Bohn, T., Avis, C.A., Beerling, D.J., Chen, G., Eliseev, A.V., Denisov, S.N., Hopcroft, P.O., Lettenmaier, D.P., Riley, W.J., Singarayer, J.S., Subin, Z.M., Tian, H., Zürcher, S., Brovkin, V., van Bodegom, P.M., Kleinen, T., Yu, Z.C., Kaplan, J.O., 2013. Present state of global wetland extent and wetland methane modelling: conclusions from a model inter-comparison project (WETCHIMP). Biogeosciences 10, 753–788.
Minasny, B., Berglund, O., Connolly, J., Hedley, C., de Vries, F., Gimona, A., Kempen, B., Kidd, D., Lilja, H., Malone, B., McBratney, A., Roudier, P., O'Rourke, S., Rudiyanto, Padarian, J., Poggio, L., ten Caten, A., Thompson, D., Tuve, C., Widyatmanti, W., 2019. Digital mapping of peatlands - a critical review. Earth Sci. Rev. 196.
Mitchell, L., Brook, E., Lee, J.E., Buizert, C., Sowers, T., 2013. Constraints on the late Holocene anthropogenic contribution to the atmospheric methane budget. Science 342, 964–966.
Murray, L.T., Mickley, L.J., Kaplan, J.O., Sofen, E.D., Pfeiffer, M., Alexander, B., 2014. Factors controlling variability in the oxidative capacity of the troposphere since the Last Glacial Maximum. Atmos. Chem. Phys. 14, 3589–3622.
National Wetlands Working Group, 1988. Wetlands of Canada. Ecological Land Classification Series, No. 24. Sustainable Development Branch, Environment Canada, Ottawa, Ontario, and Polyscience Publications Inc., Montreal, Quebec, p. 452.
Nichols, J.E., Peteet, D.M., 2019. Rapid expansion of northern peatlands and doubled estimate of carbon storage. Nat. Geosci. 12, 917–921.
Petrenko, V.V., Smith, A.M., Brook, E.J., Lowe, D., Riedel, K., Brailsford, G., Hua, Q., Schaefer, H., Reeh, N., Weiss, R.F., Etheridge, D., Severinghaus, J.P., 2009. 14CH4 measurements in Greenland ice: investigating last glacial termination CH4 sources. Science 324, 506–508.
Petrenko, V.V., Smith, A.M., Schaefer, H., Riedel, K., Brook, E., Baggenstos, D., Harth, C., Hua, Q., Buizert, C., Schilt, A., Fain, X., Mitchell, L., Bauska, T., Orsi, A., Weiss, R.F., Severinghaus, J.P., 2017. Minimal geological methane emissions during the Younger Dryas–Preboreal abrupt warming event. Nature 548, 443.
Prince, H., 1998. Wetlands of the American Midwest : A Historical Geography of Changing Attitudes. University of Chicago Press, Chicago, UNITED STATES.
Reimer, P.J., Bard, E., Bayliss, A., Beck, J.W., Blackwell, P.G., Bronk Ramsey, C., Buck, C.E., Cheng, H., Edwards, R.L., Friedrich, M., Grootes, P.M., Guilderson, T.P., Haflidason, H., Hajdas, I., Hatté, C., Heaton, T.J., Hoffmann, D.L., Hogg, A.G., Hughen, K.A., Kaiser, K.F., Kromer, B., Manning, S.W., Niu, M., Reimer, R.W., Richards, D.A., Scott, E.M., Southon, J.R., Staff, R.A., Turney, C.S.M., van der Plicht, J., 2013. IntCal13 and Marine13 radiocarbon age calibration curves 0–50,000 Years cal BP. Radiocarbon 55, 1869–1887.
Rhodes, R.H., Brook, E.J., McConnell, J.R., Blunier, T., Sime, L.C., Faïn, X., Mulvaney, R., 2017. Atmospheric methane variability: centennial-scale signals in the last glacial period. Global Biogeochem. Cycles 31, 575–590.
Ruppel, M., Väliranta, M., Virtanen, T., Korhola, A., 2013. Postglacial spatiotemporal peatland initiation and lateral expansion dynamics in North America and northern Europe. Holocene 23 (11), 1596–1606. https://doi.org/10.1177/0959683613499053.
Saunois, M., Bousquet, P., Poulter, B., Peregon, A., Ciais, P., Canadell, J.G., Dlugokencky, E.J., Etiope, G., Bastviken, D., Houweling, S., 2016. The global methane budget 2000-2012. Earth Syst. Sci. Data 8, 697.
Shur, Y.L., Jorgenson, M.T., 2007. Patterns of permafrost formation and degradation in relation to climate and ecosystems. Permafr. Periglac. Process. 18, 7–19.
Singarayer, J.S., Valdes, P.J., Friedlingstein, P., Nelson, S., Beerling, D.J., 2011. Late Holocene methane rise caused by orbitally controlled increase in tropical sources. Nature 470, 82–85.
Sowers, T., 2010. Atmospheric methane isotope records covering the Holocene period. Quat. Sci. Rev. 29, 213–221.
Swindles, G.T., Morris, P.J., Mullan, D.J., Payne, R.J., Roland, T.P., Amesbury, M.J., Lamentowicz, M., Turner, T.E., Gallego-Sala, A., Sim, T., Barr, I.D., Blaauw, M., Blundell, A., Chambers, F.M., Charman, D.J., Feurdean, A., Galloway, J.M., Gałka, M., Green, S.M., Kajukało, K., Karofeld, E., Korhola, A., Lamentowicz, Ł., Langdon, P., Marcisz, K., Mauquoy, D., Mazei, Y.A., McKeown, M.M., Mitchell, E.A.D., Novenko, E., Plunkett, G., Roe, H.M., Schoning, K., Sillasoo, Ü., Tsyganov, A.N., van der Linden, M., Väliranta, M., Warner, B., 2019. Widespread drying of European peatlands in recent centuries. Nat. Geosci. 12, 922–928. https://doi.org/10.1038/s41561-019-0462-z.
Thompson, R.L., Sasakawa, M., Machida, T., Aalto, T., Worthy, D., Lavric, J.V., Lund Myhre, C., Stohl, A., 2017. Methane fluxes in the high northern latitudes for 2005–2013 estimated using a Bayesian atmospheric inversion. Atmos. Chem. Phys. 17, 3553–3572.
Treat, C.C., Bloom, A.A., Marushchak, M.E., 2018. Non-growing season methane emissions— a significant component of annual emissions across northern ecosystems. Global Change Biol. 24, 3331–3343.
Treat, C.C., Jones, M.C., 2018. Near-surface permafrost aggradation in Northern Hemisphere peatlands shows regional and global trends during the past 6000 years. Holocene 28 (6), 998–1010. https://doi.org/10.1177/0959683617752858.
Treat, C.C., Jones, M.C., Camill, P., Gallego-Sala, A., Garneau, M., Harden, J.W., Hugelius, G., Klein, E.S., Kokfelt, U., Kuhry, P., Loisel, J., Mathijssen, P.J.H., O'Donnell, J.A., Oksanen, P.O., Ronkainen, T.M., Sannel, A.B.K., Talbot, J., Tarnocai, C., Väliranta, M., 2016. Effects of permafrost aggradation on peat properties as determined from a pan-Arctic synthesis of plant macrofossils. J. Geophys. Res.: Biogeosciences 121, 78–94.
Treat, C.C., Kleinen, T., Broothaerts, N., Dalton, A.S., Dommain, R., Douglas, T.A., Drexler, J.Z., Finkelstein, S.A., Grosse, G., Hope, G., Hutchings, J., Jones, M.C., Kuhry, P., Lacourse, T., Lähteenoja, O., Loisel, J., Notebaert, B., Payne, R.J., Peteet, D.M., Sannel, A.B.K., Stelling, J.M., Strauss, J., Swindles, G.T., Talbot, J., Tarnocai, C., Verstraeten, G., Williams, C.J., Xia, Z., Yu, Z., Väliranta, M., Hättestrand, M., Alexanderson, H., Brovkin, V., 2019. Widespread global peatland establishment and persistence over the last 130,000 y. In: Proceedings of the National Academy of Sciences, p. 201813305.
Vandenberghe, J., French, H.M., Gorbunov, A., Marchenko, S., Velichko, A.A., Jin, H., Cui, Z., Zhang, T., Wan, X., 2014. The Last Permafrost Maximum (LPM) map of the Northern Hemisphere: permafrost extent and mean annual air temperatures, 25–17 ka BP. Boreas 43, 652–666.
Walter Anthony, K.M., Zimov, S.A., Grosse, G., Jones, M.C., Anthony, P.M., Iii, F.S.C., Finlay, J.C., Mack, M.C., Davydov, S., Frenzel, P., Frolking, S., 2014. A shift of thermokarst lakes from carbon sources to sinks during the Holocene epoch. Nature 511, 452–456.
Walter, K.M., Edwards, M.E., Grosse, G., Zimov, S.A., Chapin, F.S., 2007. Thermokarst lakes as a source of atmospheric CH4 during the last deglaciation. Science 318, 633–636.
Webster, K.L., Bhatti, J.S., Thompson, D.K., Nelson, S.A., Shaw, C.H., Bona, K.A., Hayne, S.L., Kurz, W.A., 2018. Spatially-integrated estimates of net ecosystem exchange and methane fluxes from Canadian peatlands. Carbon Bal. Manag. 13, 16.
Wik, M., Varner, R.K., Anthony, K.W., MacIntyre, S., Bastviken, D., 2016. Climate-sensitive Northern Lakes and Ponds Are Critical Components of Methane Release. Nature Geosci advance online publication.
Xu, J., Morris, P.J., Liu, J., Holden, J., 2018. PEATMAP: refining estimates of global peatland distribution based on a meta-analysis. Catena 160, 134–140.
Xu, X., Yuan, F., Hanson, P.J., Wullschleger, S.D., Thornton, P.E., Riley, W.J., Song, X., Graham, D.E., Song, C., Tian, H., 2016. Reviews and syntheses: four decades of modeling methane cycling in terrestrial ecosystems. Biogeosciences 13, 3735–3755.
Yu, Z., Loisel, J., Turetsky, M.R., Cai, S., Zhao, Y., Frolking, S., MacDonald, G.M., Bubier, J.L., 2013. Evidence for elevated emissions from high-latitude wetlands contributing to high atmospheric CH4 concentration in the early Holocene. Global Biogeochem. Cycles 27, 131–140.